Journal of Gerontology: BIOLOGICAL SCIENCES
Cite journal as: J Gerontol A Biol Sci Med Sci
2010 Vol. 65A, No. 2, 147–155
doi:10.1093/gerona/glp203

Advance Access published on January 7, 2010

Possible Molecular Mechanisms Underlying Age-Related Cardiomyocyte Apoptosis in the F344XBN Rat Heart

Sunil K. Kakarla,[1] Kevin M. Rice[2,3] Anjaiah Katta,[1] Satyanarayana Paturi[2,3] Miaozong Wu[2,3] Madhukar Kolli,[2] Saba Keshavarzian,[2] Kamran Manzoor,[4] Paulette S. Wehner,[5] and Eric R. Blough[1–3,6]

[1]Department of Pharmacology, Physiology, and Toxicology, Joan C. Edwards School of Medicine. [2]Department of Biological Sciences, and [3]Cell Differentiation and Development Center, Marshall University, Huntington, West Virginia.
[4]Charleston Area Medical Center, West Virginia.
[5]Department of Cardiology, Joan C. Edwards School of Medicine and [6]Division of Exercise Science, Sport and Recreation, College of Education and Human Services, Marshall University, Huntington, West Virginia.

Despite advances in treatment, age-related cardiac dysfunction still remains a leading cause of cardiovascular death. Recent data have suggested that increases in cardiomyocyte apoptosis may be involved in the pathological remodeling of heart. Here, we examine the effects of aging on cardiomyocyte apoptosis in 6-, 30-, and 36-month-old Fischer344xBrown Norway F1 hybrid rats (F344XBN). Compared with 6-month hearts, aged hearts exhibited increased TdT-mediated dUTP nick end labeling–positive nuclei, caspase-3 activation, caspase-dependent cleavage of α-fodrin and diminished phosphorylation of protein kinase B/Akt (Thr 308). These age-dependent increases in cardiomyocyte apoptosis were associated with alterations in the composition of the cardiac dystrophin glycoprotein complex and elevated cytoplasmic IgG and albumin immunoreactivity. Immunohistochemical analysis confirmed these data and demonstrated qualitative differences in localization of dystrophin–glycoprotein complex (DGC) molecules with aging. Taken together, these data suggest that aging-related increases in cardiac apoptotic activity model may be due, at least in part, to age-associated changes in DGC structure.

Key Words: Aging—Cardiac declines with age—Dystroglycan—Apoptosis—Cellular senescence.

ADVANCING age is associated with increased risk of cardiovascular disease and a progressive decrease in cardiac function (1). Recent investigation using the Fischer 344xBrown Norway F1 hybrid (F344XBN) rat model has demonstrated similar changes as aging in these animals is associated with an increased incidence of cardiac arrhythmias as well as impairment of systolic and diastolic function (2,3). In addition, other data have shown that the aged F344XBN heart exhibits increased expression of oxidative–nitrosative stress markers (4). Reactive oxygen species (ROS) such as superoxide anions ($\bullet O_2^-$) and hydroxy radicals (•OH) have been implicated in cardiac dysfunction, remodeling, and in cardiomyocyte apoptosis (5). Whether aging in the F344XBN heart is associated with changes in cardiac apoptosis is not well understood.

The dystrophin–glycoprotein complex (DGC) is located within the cell membrane and provides a strong mechanical link between the cell cytoskeleton and the extracellular matrix (6). In cardiac muscle, disruption of DGC may be involved in mediating contractile dysfunction, the development of arrhythmias, and the progression of cardiac hypertrophy (7–14). How the cardiac DGC may be affected by aging and whether changes in the DGC may be related to increases in cardiac apoptosis have not been elucidated. Known components of the DGC include dystrophin, dystroglycans, sarcoglycans, integrins, caveolin-3, and others. The regulation of these proteins differs depending on muscle type (15) and is altered, at least in skeletal muscle, with aging (16). Here, we hypothesized that aged F344XBN hearts exhibited age-related changes in cardiac function and morphology (3,4) and would also exhibit increases in cardiac apoptosis and that this finding would be associated with alterations in the expression and localization of DGC proteins. Although incapable of proving cause and effect, the data of the present study suggest that alterations to the cardiac DGC may be implicated in the pathogenesis of age-related cardiac dysfunction.

Materials and Methods

Animals

Animal care and procedures were conducted in accordance with the Animal Use Review Board of Marshall University using the criteria outlined by the American Association of Laboratory Animal Care (AALAC) as proclaimed in the Animal Welfare Act (PL89-544, PL91-979, and PL94-279). The animals and tissues used in this study have been previously examined (3,4). Adult (6 months, $n = 8$), aged (30 months, $n = 8$), and very aged (36 months, $n = 8$) male F344XBN rats were obtained from the National Institute on Aging. Rats were housed two per cage in an AALAC-approved vivarium. Housing conditions consisted of a 12 hour:12 hour dark–light cycle with temperature maintained at 22 ± 2°C. Animals were provided food and water ad libitum. Rats were allowed to acclimate to the housing facilities for at least 2 weeks before experimentation began. During this time, the animals were carefully observed and weighed weekly. None of the animals exhibited signs of failure to thrive, such as precipitous weight loss, disinterest in the environment, or unexpected gait alterations.

Materials

Antibodies used were dystrophin (dys-2) from Novacastro (Ontario, Canada); α-dystroglycan (sc-28534), β-dystroglycan (sc16165), β-sarcoglycan (Sc-28279), and δ-sarcoglycan (Sc-28281) were from Santa Cruz (Santa Cruz, CA); α-sarcoglycan (VP-A105) from Vector Laboratories (Burlingame, CA); rat albumin (ab53435) from Abcam; and rat IgG antibody (T6392) from Molecular Probes (Eugene, OR). Caspase 3 (9662), caspase 9 (9506), α-fodrin (2122), Akt (9272), Thr^{308} phosphorylated Akt (9275), anti-rabbit (7074) and anti-mouse (7076) IgG secondary antibodies were purchased from Cell Signaling Technology (Beverly, MA). The In Situ Cell Death Detection Kit, Fluorescein (TdT-mediated dUTP nick end labeling [TUNEL]) was from Roche Diagnostics (Mannheim, Germany). Precast 10% sodium dodecyl sulfate–polyacrylamide gel electrophoresis (SDS-PAGE) gels were procured from Cambrex Biosciences (Baltimore, MD), and enhanced chemiluminescence (ECL) Western blotting detection reagent was from Amersham Biosciences (Piscataway, NJ). Restore Western blot stripping buffer was obtained from Pierce (Rockford, IL); 3T3 and L6 cell lysates were from Santa Cruz Biotechnology (Santa Cruz, CA). All other chemicals were purchased from Sigma (St. Louis, MO).

Cardiac Morphology

Animals were anesthetized with an intraperitoneal injection of ketamine (40 mg/kg) and xylazine (10 mg/kg), supplemented as necessary for reflexive response. Hearts were quickly removed, blotted dry, weighed, and immediately frozen in liquid nitrogen before storing at −80°C until use. Histological imaging and immunohistochemistry were performed on hearts sectioned (8 μm) using an IEC Minotome cryostat and collected on polylysine-coated slides (Sigma). Sections were stained with mallory phosphotungstic acid hematoxylin (PTAH) staining as outlined by the manufacturer (Poly Scientific R & D Corp., Bay Shore, NY) for the evaluation of cardiac morphology. Immunostaining for dystrophin, rat IgG, and albumin was performed as outlined by the antibody manufacturer. Briefly, sections were incubated for 30 minutes in a blocking solution (5% bovine serum albumin [BSA] and phosphate-buffered saline [PBS] containing 0.5% Tween 20 (PBS-T), pH 7.5) and then incubated with specific antisera diluted in PBS-T (anti-dystrophin 1:100, rat-IgG 1:100) for 1 hour at 37°C in a humidified chamber. After washing in PBS-T (3 × 5 minutes), sections were incubated with the appropriate FITC or Texas RED labeled secondary antibody (1:200), if appropriate, for 1 hour at 37°C in a humidified chamber. After mounting, specimens were visualized by epifluorescence using an Olympus fluorescence microscope (Melville, NY) fitted with a ×40 objective or on a Nikon Diaphot microscope (Bio-Rad, Hercules, CA) for confocal analysis. To allow approximate qualitative comparisons, all imaging parameters were kept constant between samples.

TUNEL Staining

DNA fragmentation after staining for dystrophin was determined by TUNEL according to the manufacturer's recommendations. TUNEL staining was performed on tissue sections (8 μm) obtained from 6-month ($n = 3$), 30-month ($n = 3$), and 36-month ($n = 3$) hearts, which were fixed with 4% paraformaldehyde, washed with PBS (pH 7.4), and then permeabilized with 0.1% sodium citrate and 0.1% Triton-X. Additional experiments performed in parallel using DNase I or the omission of labeling reagent were used as positive and negative controls. Three randomly selected regions from each cross section were visualized by epifluorescence using an Olympus fluorescence microscope fitted with a ×20 objective. Images were recorded digitally using a CCD camera (Olympus).

Protein Isolation and Immunoblotting

For the preparation of protein isolates, heart tissues were pulverized in liquid nitrogen using a mortar and pestle and washed three times with ice-cold PBS. Cytoplasmic proteins were extracted under mild conditions by incubating samples on ice in 2 μl/mg of T-PER (Pierce) protein extraction reagent that had been supplemented with (1.50 mM $MgCl_2$, 1 mM EDTA, 1 μg/mL aprotinin, 1 μg/mL leupeptin, 1 μg/mL pepstatin, 1 mM phenylmethanesulphonylfluoride (PMSF), 1 mM Na_3VO_4) for 5 minutes. After centrifugation (10 minutes at 800*g*), the supernant was removed and the pellets were re-extracted twice. Membrane proteins were obtained by resuspending the pellet from the previous cytoplasmic extraction from the pulverized heart tissues (1 mL/g) in a buffer containing 1% deoxycholate, 1% NP-40, 10 mM $NaPO_4$, 140 mM NaCl, and 2 mM EDTA supplemented with 100 mM NaF, 1 mM Na_3VO_4, 2 mM PMSF, 1 μg/mL aprotinin, 1 μg/mL leupeptin, and 1 μg/mL pepstatin. After collecting the supernatant by centrifugation for 10 minutes at 800*g*, protein concentration was determined in triplicate via the Bradford method (Pierce) using BSA as a standard. Samples were analyzed using 10% SDS-PAGE. To allow direct comparisons between age groups, 30 μg of samples from different age groups were loaded into consecutive wells of the same gel and ran. Following electrophoresis, proteins were transferred onto Hybond nitrocellulose membranes (Amersham Biosciences) using standard conditions (17). Membranes were stained with Ponceau S, and the amount of protein quantified by densitometric analysis to confirm successful transfer of proteins and equal loading of lanes as described previously (18–20). Membranes were blocked in tris-buffered saline (TBS) with 0.5% Tween 20 (TBS-T) and 5% milk for 1 hour at room temperature, washed (TBS-T, 3 × 5 minutes), and incubated in primary antibody overnight at 4°C or 1 hour at room temperature as outlined by the antibody manufacturer. Immunoreactive protein bands were visualized by ECL Western blotting detection reagent. Film exposure time was adjusted to keep the integrated optical densities (IODs) within a linear and non-saturated range, and band intensity was quantified by

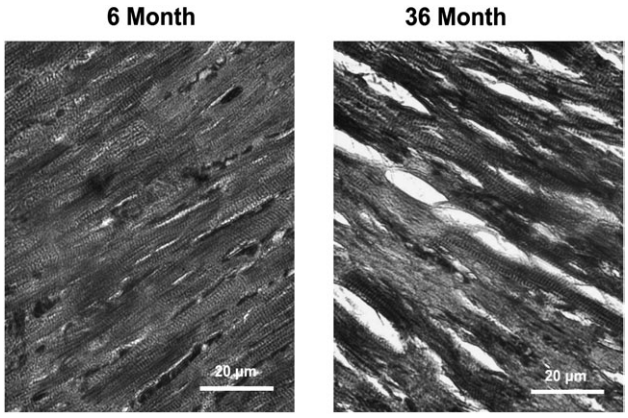

Figure 1. Aging alters the morphology of cardiac tissue in the F344XBN heart. Cross sections of hearts obtained from adult (6-month) and very aged (36-month) rats after staining with phosphotungstic acid hematoxylin to visualize cardiac morphology. Bar = 20 µm.

densitometry using a flatbed scanner (Epson Perfection 3200 PHOTO scanner, Epson America Inc., Long Beach, CA) and imaging software (AlphaEaseFC, Alpha Innotech, San Leandro, CA). Immunoblots were stripped with Restore Western blot stripping buffer as outlined previously (21).

Statistical Analysis

Results are presented as mean ± *SEM*. Data were analyzed by using SigmaStat 3.0 (Systat Software Inc., Point Richmond, CA) computer software. One-way analysis of variance (22) was used for overall comparisons, with the Student-Newman-Keuls post hoc test used to determine statistical significance. The level of significance accepted a priori was $p \leq .05$.

Results

As reported previously (3,4), the body weight, heart weight, and body weight to heart weight ratios of these animals were increased in 30- and 36-month compared with 6-month animals ($p < .05$). PTAH staining of 6-month hearts demonstrated distinct myocyte striations, whereas very aged hearts showed presence of connective tissue infiltration and loss of myocytes (Figure 1).

Aging in the F344XBN Heart is Associated With Increased TUNEL Positive Nuclei, Elevated Caspase-3 Activation, and Diminished Akt Phosphorylation

To investigate the possibility that aging was associated with an increase in cardiac apoptosis, we examined the number of nuclei staining positively for DNA fragmentation by TUNEL staining. Compared with 6-month hearts, the number of TUNEL positive nuclei appeared to be markedly increased in 30- and 36-month hearts (Figure 2).

A critical step in the execution of the apoptotic program that elicits DNA fragmentation is cleavage of caspase-3 into 19 and 17 kDa fragments (23). Caspases are

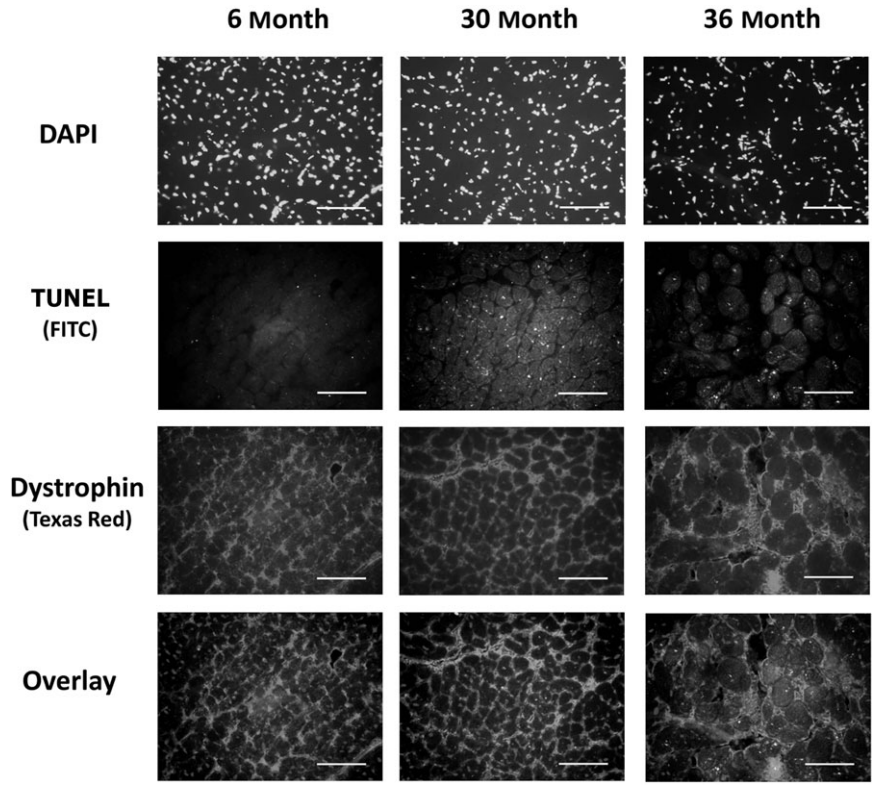

Figure 2. Aging increases the number of apoptotic nuclei in cardiomyocytes. TdT-mediated dUTP nick end labeling [TUNEL] staining along with immunostaining for dystrophin (Texas Red) was used to investigate myocytes apoptosis in 6-, 30-, and 36-month hearts. Bar = 50 µm.

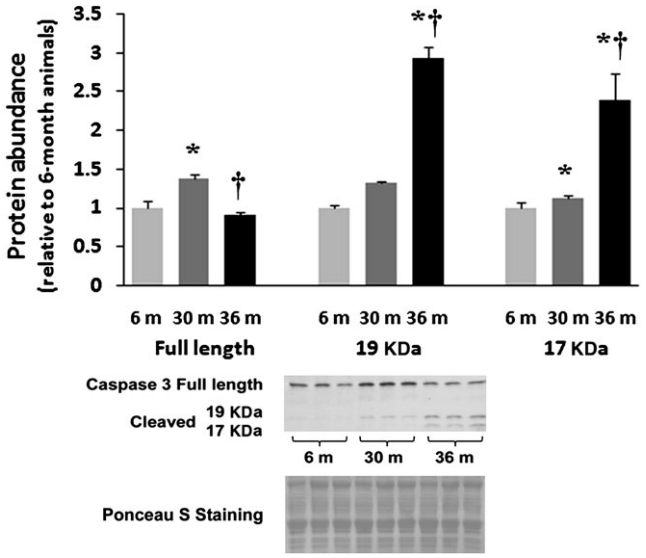

Figure 3. Aging increases the cleavage of caspase-3. Protein isolates from cytosolic fraction of hearts excised from adult (6-month), aged (30-month), and very aged (36-month) rats were analyzed by immunoblotting for changes in caspase-3 and caspase-3 cleavage. Ponceau S staining of the nitrocellulose membrane along with densitometric analysis of protein present was done to verify equivalent protein loading between the lanes (data not shown). Asterisk indicates significant difference from adult (6-month) value ($p < .05$). Dagger indicates significant difference from 30-month value ($p < .05$). $n = 8$ for all groups.

cysteine-dependent aspartate-specific proteases functioning as endonucleases integral in the final execution of nuclei and cell death (23,24). With aging, the amount of full-length (inactive) caspase-3 was 39% higher ($p < .05$) in 30-month hearts, whereas it was 10% lower in 36-month hearts as compared with 6-month hearts (Figure 3; $p < .05$). Caspase-3 cleavage into 17 kDa fragments was markedly higher (139%, $p < .05$) in the 36-month hearts compared with that observed in 6-month animals (Figure 3). Similarly, the 19-kDa fragment of caspase-3 was also 32% ($p < .05$) and 192% ($p < .05$) higher in the 30- and 36-month hearts, respectively (Figure 3).

To examine the upstream signaling events responsible for caspase-3 activation, we next investigated the regulation of the caspase-9. Caspase-9 is cleaved and activated via mitochondrial cytochrome c release (25). Full-length (inactive) caspase-9 content was 31% higher in 36-month hearts ($p < .05$) compared with 6-month hearts (Figure 4). The 40-kDa fragment of caspase-9 was higher (35%) in 36-month hearts ($p < .05$), with no significant difference between 6- and 30-month hearts (Figure 4).

As a means of further verifying the activation of caspase-3, we also examined the effects of aging on the cleavage of α-fodrin. α-Fodrin is a cytoskeletal protein which undergoes caspase-dependent proteolytic processing in many types of cell death (26) but has not, to our knowledge, been studied in aging cardiac muscle. Compared with 6-month animals, the amount of α-fodrin was 14% lower in 30-month hearts (Figure 4). The full-length 240-kDa α-fodrin protein can be cleaved at several sites within its sequence by activated calpains to yield an N-terminal fragment of 150 kDa or by caspases to yield a C-terminal 120 kDa product (27,28). Compared with hearts obtained from 6-month animals, the amount of the caspase-dependent (120 kDa) form of α-fodrin cleavage was 24% lower ($p < .05$) in 30-month and 17% higher ($p < .05$) in 36-month hearts (Figure 4). The calpain-dependent (150-kDa) fragment of α-fodrin cleavage was undetectable.

The Akt/PKB is a serine/threonine protein kinase that functions as a critical regulator of cell survival and proliferation through numerous antiapoptotic actions (29). Given our findings of increased TUNEL positive nuclei, we hypothesized that aging would be associated with reduced Akt expression. The content of Akt was 28% and 14% lower ($p < .05$) in 30- and 36-month hearts compared with 6-month hearts (Figure 4). Furthermore, Akt phosphorylation (Thr 308) was reduced by 24% and 26% ($p < .05$) in the 30- and 36-month hearts, respectively (Figure 4). Taken together, these data suggest that aging in the F344XBN heart is associated with increased cardiomyocyte apoptosis.

Aging in the F344XBN Heart is Associated With Alterations in the Cardiac DGC and Cardiac Membrane Integrity

Immunoblots of protein isolates obtained from the cytosolic and membrane fraction of 6-, 30-, and 36-month hearts were examined for the relative abundance of dystrophin. Compared with 6-month animals, the amount of cytoplasmic dystrophin protein was 26% and 23% higher ($p < .05$) in 30- and 36-month hearts, respectively (Figure 5A). Relative to 30-month animals, the amount of dystrophin in the membrane fraction was 44% less ($p < .05$) in 36-month animals. To assess the subcellular distribution of dystrophin, tissue sections from hearts of differently aged animals were examined by immunohistochemistry. Antibodies directed against the COOH terminus of dystrophin showed uniform immunoreactivity located predominantly along the cell membrane in the 6-month heart (Figure 5B). In comparison, dystrophin immunoreactivity in 30- and 36-month heart fibers appeared irregular with patches of intense fluorescence. With aging, the dystrophin immunoreactivity often appeared to be discontinuous and was at times completely absent along the sarcolemma (Figure 5B).

Because alterations in the amount of dystrophin may influence the composition of the DGC, we next examined whether aging may affect the regulation of dystroglycans and sarcoglycans. Compared with 6-month animals, immunoblot analysis showed that the amount of α-dystroglycan was 44% and 74% higher in cytosol and 16% and 23% higher in membrane fraction of 30- and 36-month hearts, respectively ($p < .05$) (Figure 6A), indicating that the amount of α-dystroglycan being localized to sarcolemma

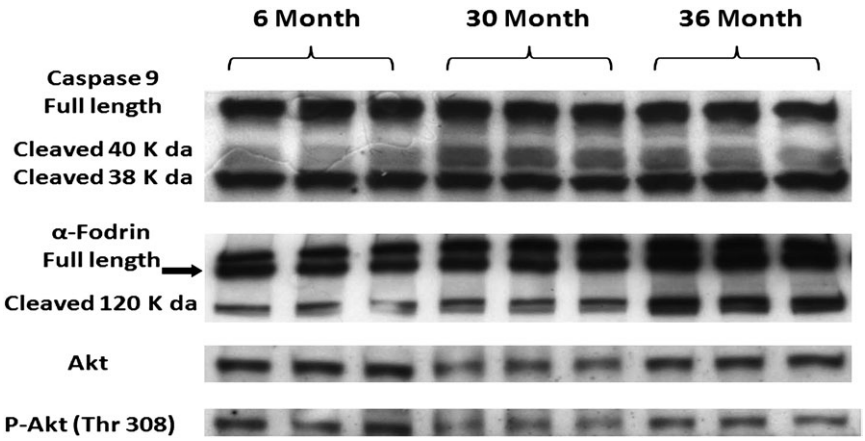

Figure 4. Aging alters the regulation of mitochondrial dependent apoptotic pathway signaling proteins. Protein isolates from cytosolic fraction of hearts excised from adult (6-month), aged (30-month), and very aged (36-month) rats were analyzed by immunoblotting for changes in caspase-9, α-fodrin, Akt, and Akt phosphorylation (Thr308). Ponceau S staining of the nitrocellulose membrane along with densitometric analysis of protein present was done to verify equivalent protein loading between the lanes (data not shown). $n = 8$ for all groups.

was diminished with aging. Compared with 6-month hearts, the amount of cytosolic β-dystroglycan was 36% and 37% lower in 30- and 36-month hearts, respectively ($p < .05$; Figure 6B). In contrast, the amount of membrane β-dystroglycan was unchanged and 58% higher ($p < .05$) in 30- and 36-month hearts compared with that observed in 6-month old animals (Figure 6B). Immunoblot analysis using an antibody to a glycosylated epitope showed that the cardiac muscle membrane content of α-sarcoglycan was slightly decreased by 8.5% and 14%, respectively ($p < .05$) in 30- and 36-month

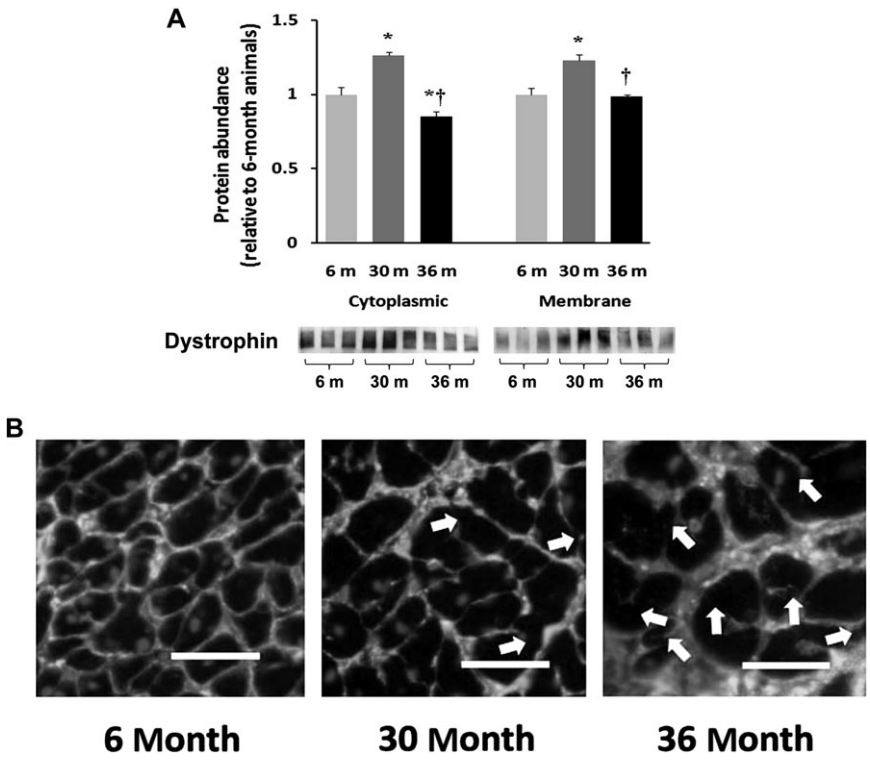

Figure 5. Aging alters the regulation of dystrophin in the F344XBN heart. **A**). Protein isolates from cytoplasmic and membrane fractions of hearts obtained from adult (6-month), aged (30-month), and very aged (36-month) rats were analyzed by immunoblotting for changes in dystrophin protein content. Ponceau S staining of the nitrocellulose membrane along with densitometric analysis of protein present was done to verify equivalent protein loading between the lanes (data not shown). Asterisk indicates significant difference from adult (6-month) value ($p < .05$). Dagger indicates significant difference from 30-month value ($p < .05$). $n = 8$ for all groups. **B**). Dystrophin immunofluorescence in 6-, 30-, and 36-month hearts. Arrows indicate irregular and discontinuous immunoreactive signaling along the sarcolemma in the 30- and 36-month hearts. Bar = 50 μm.

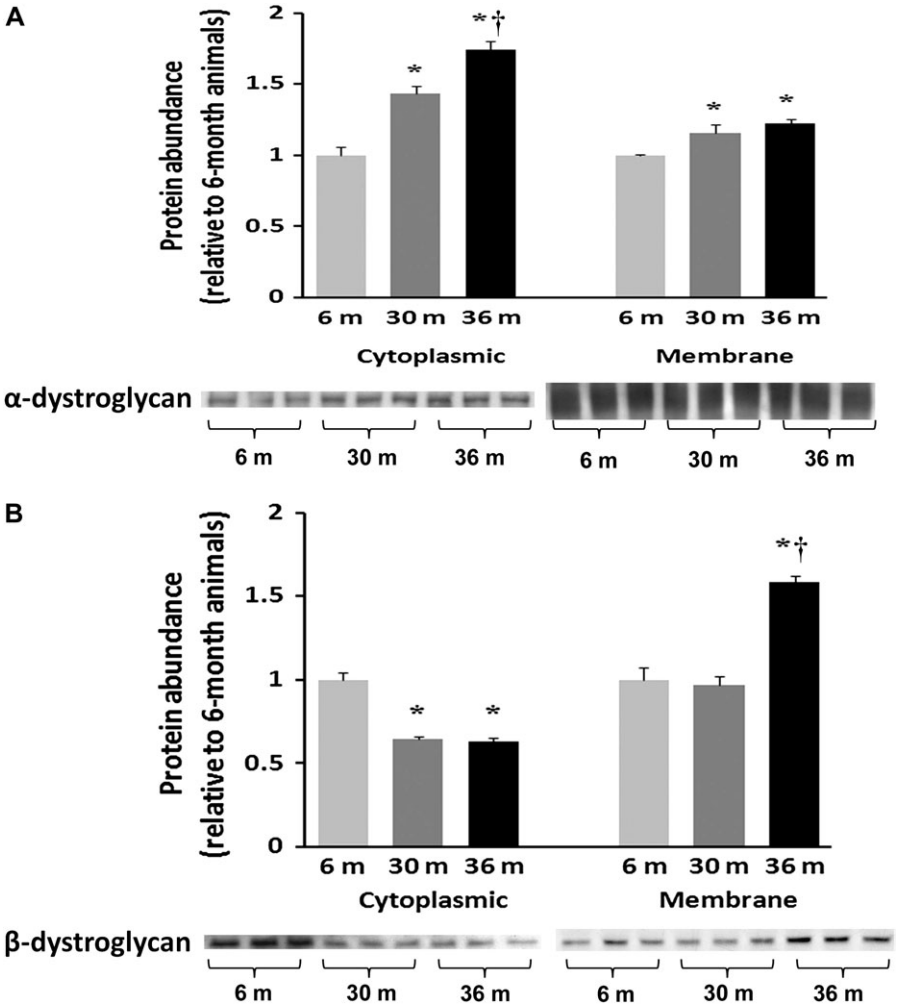

Figure 6. Aging alters the regulation of dystroglycans in the F344XBN heart. Protein isolates from cytoplasmic and membrane fractions of hearts excised from adult (6-month), aged (30-month), and very aged (36-month) rats were analyzed by immunoblotting for changes in (**A**) α-dystroglycan and (**B**) β-dystroglycan protein expression. Ponceau S staining of the nitrocellulose membrane along with densitometric analysis of protein present was done to verify equivalent protein loading between the lanes (data not shown). Asterisk indicates significant difference from adult (6-month) value ($p < .05$). Dagger indicates significant difference from 30-month muscles ($p < .05$). $n = 8$ for all groups.

hearts compared with 6-month animals (Figure 7). Similarly, membrane β-sarcoglycan content was reduced by 12% and 16% in 30- and 36-month hearts, respectively ($p < .05$; Figure 7). Likewise, compared with 6-month hearts, the amount of δ-sarcoglycan was reduced by 28% and 19% in 30- and 36-month hearts, respectively, ($p < 0.05$; Figure 7). Together, these data suggest that aging in the F344XBN heart is associated with changes in the composition of the cardiac DGC.

Because DGC is known to play a pivotal role in stabilizing the muscle cell membrane and changes in cardiomyocyte membrane permeability are associated with cellular apoptosis (30), we next examined whether alterations in the DGC complex were associated with evidence of increased membrane permeability. To test this possibility, tissue sections obtained from 6-, 30-, and 36-month rat hearts were examined for the presence of IgG (150 kDa), a serum protein, and albumin, a plasma constituent that is normally excluded from entry into the muscle fiber. No evidence of IgG (Figure 8A) and albumin (Figure 8B) immunoreactivity was demonstrated in the cytosol of cardiac muscle fibers obtained from

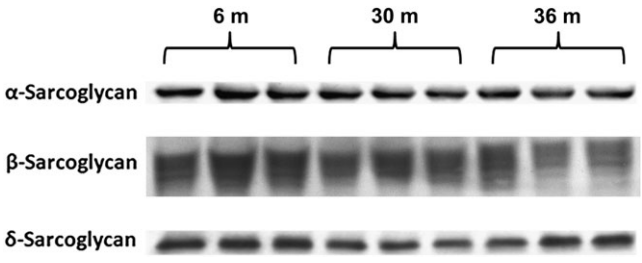

Figure 7. α-, β-, and δ-sarcoglycan protein levels are altered with aging. Protein isolates excised from adult (6-month), aged (30-month), and very aged (36-month) rats were analyzed by immunoblotting for α-, β-, and δ-sarcoglycan protein expression. $n = 8$ for all groups.

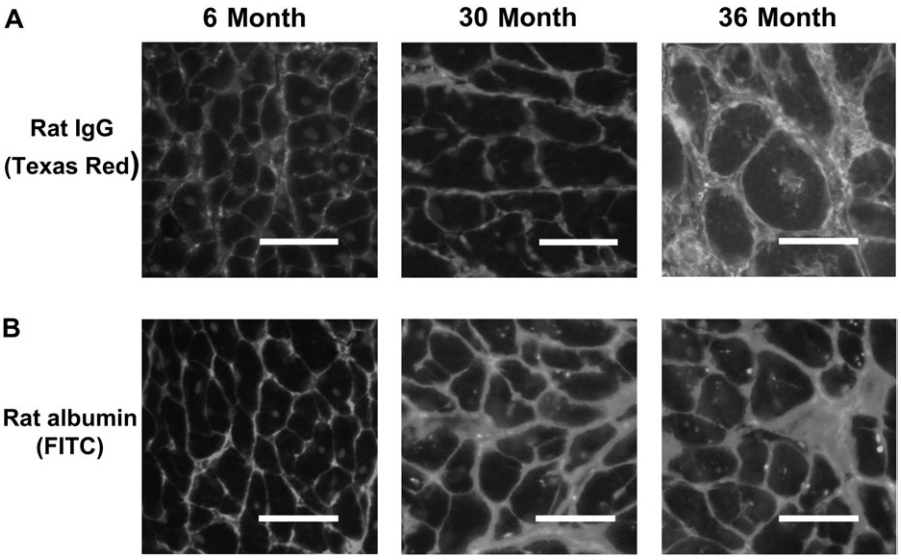

Figure 8. Aging is associated with a loss of cardiac myocyte membrane integrity. **A**). Double immunofluorescence labeling with dystrophin (FITC) and rat IgG (Texas Red) in 6-, 30-, and 36-month hearts. Increased permeability of the myocytes membrane is indicated by intracellular IgG reactivity. Note diffuse immunoreactive signaling within the cytoplasm of the 30- and 36-month hearts. **B**). Immunofluorescent labeling with anti-rat albumin in 6-, 30-, and 36-month hearts. Note localization of albumin in 30- and 36-month hearts. Bar = 50 μm.

6-month rats. In contrast, very aged rats exhibited positive staining with anti-rat IgG and anti-rat albumin antibodies in the cytoplasm of cardiac myofibers obtained from 36-month rats (Figure 8A and B). This finding consistent with the notion that aging in the F344XBN heart is associated with increased cardiomyocyte permeability.

Discussion

In the present investigation, we examined how aging may affect cardiomyocyte apoptosis in the hearts of animals that have previously been shown by echocardiography to exhibit age-related dysfunction and biochemically to exhibit increased oxidative–nitrosative stress (3,4). Here, we demonstrate that aging in the F344XBN rat heart is associated with changes in cardiac morphology and an increase in the number of TUNEL positive cells (Figures 1 and 2). These data, considered in concert with our previous findings, suggest that aging-associated increases in oxidative–nitrosative stress may be related to cardiomyocyte loss.

In order to investigate potential mechanisms of the apoptosis observed in our TUNEL studies, we determined how aging affected the expression and activation of two key effectors of mitochondrial-mediated apoptosis, caspase-3 and -9 (31–33). With advanced aging, we observed increases in the amount of cleaved caspase-3 and its upstream activator, caspase-9 (Figures 3 and 4). Supporting the possibility that caspase-3 activation occurs with aging, we also observed that the amount of caspase-cleaved α-fodrin content was increased with advanced aging (Figure 4). Taken together, these data support the notion that the mitochondrial apoptotic cascade may contribute to apoptosis in the aging F344XBN heart. This is in agreement with the results of other recent investigations that have implicated mitochondrial-mediated apoptosis in the loss of cardiomyocytes with aging (34,35). In addition to increased proapoptotic caspase activity, we also demonstrate that age-related increases in the cardiac apoptosis in the F344XBN are associated with decreased phosphorylation of Akt (Figure 4). Why Akt phosphorylation may be decreased with aging is currently unclear.

Alterations to the muscle DGC and how these changes may influence muscle morphology or function have been well examined in the muscular dystrophies (36,37). Duchenne and Becker muscular dystrophies are associated with a high incidence of dilated cardiomyopathy (7,38), and dystrophin mutations are a cause of X-linked dilated cardiomyopathy (12,39). These observations suggest that structural and functional impairments of DGC may serve to promote cardiac dysfunction (40). Thus, we hypothesized that age-related disruptions of cardiac DGC function may be partially responsible for the degenerative role of normative aging on heart function. One of the main findings of the present study is that aging in the F344XBN rat heart is associated with alterations in the expression levels of dystrophin (Figure 5), dystroglycans (Figure 6), and sarcoglycans (Figure 7). Interestingly, the regulation of these proteins appears to occur in a diametric fashion. For example, although the amount of α-, β-dystroglycan protein levels increases in the membrane fraction with aging, the amount of dystrophin and the α-, β-, and δ-sarcoglycans decrease. It has been hypothesized that β-dystroglycan acts as a link between proteins in the DGC complex and the extracellular matrix (41). Thus, it is tempting to speculate that the age-associated upregulation of

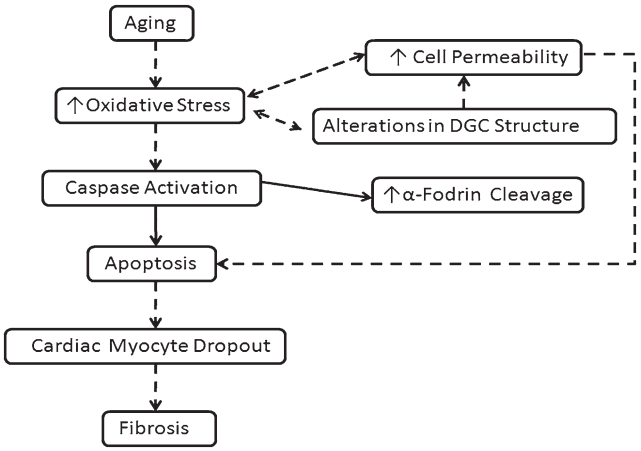

Figure 9. Proposed model for how changes in the dystrophin–glycoprotein complex (DGC) may be related to age-related cardiac dysfunction. Data from the literature support the existence of increased oxidative stress and contractile dysfunction in aged cardiac muscle. Changes in the cardiac DGC could contribute to each of these processes either directly or by causing changes in cell permeability or by increasing myocyte apoptosis. Dashed arrows indicate cellular mechanisms that have been postulated to participate where as solid arrows indicate measures that were experimentally assessed in this study.

the dystroglycans that we show may represent an attempt by the cardiomyocyte to "re-establish" a functional connection between the cell cytoskeleton and the extracellular matrix. Although not examined here, it is interesting to note that previous work has demonstrated that inhibition of α-dystroglycan binding to laminin-2 is associated with diminished Akt phosphorylation and the induction of apoptosis in muscle cell cultures (42). Whether the decreased phosphorylation of Akt we observe in the aging F344XBN heart is due to alterations in the interaction between α-dystroglycan and laminin-2 or some other mechanism will require further investigation.

Although the exact function of DGC is not fully understood, it is known to regulate the structural stability of the muscle cell membrane. Indeed, alterations in dystroglycan or sarcoglycan levels have been shown to cause muscle membrane instability (43,44), and cardiomyocytes lacking dystrophin are abnormally vulnerable to mechanical stress–induced injury causing loss of sarcolemmal integrity and myofibrillar degeneration that can lead to contractile dysfunction (6,45). Our findings of increased intracellular cytoplasmic IgG and albumin immunoreactivity in the aged F344XBN hearts (Figure 8) are consistent with this notion. This destabilization of the membrane, in turn, has been linked to increased cellular apoptosis (42,46), which is in agreement with our finding of increased cardiomyocyte apoptosis with aging. Whether changes in the DGC precede elevations in cardiac ROS and apoptosis or if alterations in cardiac ROS and apoptosis occur prior to modification of the DGC is not known and, unfortunately, cannot be determined from the present data. Future studies using cultured cardiomyocytes and siRNAs to alter expression of different DGC proteins may be useful in increasing our understanding of the cause and effect relationship between cardiomyocyte apoptosis and age-related changes in DGC.

In summary, this study demonstrates that aging in the F344XBN rats is characterized by increased cardiomyocyte apoptosis and alterations in the expression and localization of cardiac DGC proteins. Although not capable of proving cause and effect, these data when considered in conjunction with our previous reports are consistent with the possibility that age-associated increases in cardiac dysfunction, oxidative–nitrosative stress, and apoptotic activity in the F344XBN aging model may be due, at least in part, to age-related changes in DGC structure and function (Figure 9) (3,4). Further experiments using other time points within the aging spectrum and other types of analysis will no doubt be useful in determining if this venue is worth exploring.

Funding

This study was supported by National Institutes of Health Grant No. AG-027103 to E.R.B.

Correspondence

Address correspondence to Eric R. Blough, PhD, Laboratory of Molecular Physiology, Suite 311, Room 241N, Robert C. Byrd Biotechnology Science Center, Department of Biological Sciences, 1700 3rd Avenue, Marshall University, Huntington, WV 25755-1090. Email: blough@marshall.edu

References

1. Lakatta EG. Aging and cardiovascular structure and function in healthy sedentary humans. *Aging (Milano)*. 1998;10:162–164.
2. Hacker TA, McKiernan SH, Douglas PS, Wanagat J, Aiken JM. Age-related changes in cardiac structure and function in Fischer 344 x Brown Norway hybrid rats. *Am J Physiol Heart Circ Physiol*. 2006; 290:H304–H311.
3. Walker EM, Jr., Nillas MS, Mangiarua EI et al. Age-associated changes in hearts of male Fischer 344/Brown Norway F1 rats. *Ann Clin Lab Sci*. 2006;36:427–438.
4. Asano S, Rice KM, Kakarla S et al. Aging influences multiple indices of oxidative stress in the heart of the Fischer 344/NNia x Brown Norway/BiNia rat. *Redox Rep*. 2007;12:167–180.
5. Tsutsui H, Ide T, Kinugawa S. Mitochondrial oxidative stress, DNA damage, and heart failure. *Antioxid Redox Signal*. 2006;8:1737–1744.
6. Lapidos KA, Kakkar R, McNally EM. The dystrophin glycoprotein complex: signaling strength and integrity for the sarcolemma. *Circ Res*. 2004;94:1023–1031.
7. Beggs AH. Dystrophinopathy, the expanding phenotype. Dystrophin abnormalities in X-linked dilated cardiomyopathy. *Circulation*. 1997;95:2344–2347.
8. Frank JS, Mottino G, Chen F, Peri V, Holland P, Tuana BS. Subcellular distribution of dystrophin in isolated adult and neonatal cardiac myocytes. *Am J Physiol*. 1994;267:C1707–C1716.
9. Hein S, Kostin S, Heling A, Maeno Y, Schaper J. The role of the cytoskeleton in heart failure. *Cardiovasc Res*. 2000;45:273–278.
10. Keller RS, Shai SY, Babbitt CJ et al. Disruption of integrin function in the murine myocardium leads to perinatal lethality, fibrosis, and abnormal cardiac performance. *Am J Pathol*. 2001;158:1079–1090.
11. Kostin S, Hein S, Arnon E, Scholz D, Schaper J. The cytoskeleton and related proteins in the human failing heart. *Heart Fail Rev*. 2000;5: 271–280.

12. Ortiz-Lopez R, Li H, Su J, Goytia V, Towbin JA. Evidence for a dystrophin missense mutation as a cause of X-linked dilated cardiomyopathy. *Circulation*. 1997;95:2434–2440.
13. Petrof BJ, Shrager JB, Stedman HH, Kelly AM, Sweeney HL. Dystrophin protects the sarcolemma from stresses developed during muscle contraction. *Proc Natl Acad Sci U S A*. 1993;90:3710–3714.
14. Wang J, Hoshijima M, Lam J et al. Cardiomyopathy associated with microcirculation dysfunction in laminin alpha4 chain-deficient mice. *J Biol Chem*. 2006;281:213–220.
15. Wheeler MT, Allikian MJ, Heydemann A, McNally EM. The sarcoglycan complex in striated and vascular smooth muscle. *Cold Spring Harb Symp Quant Biol*. 2002;67:389–397.
16. Rice KM, Preston DL, Neff D, Norton M, Blough ER. Age-related dystrophin-glycoprotein complex structure and function in the rat extensor digitorum longus and soleus muscle. *J Gerontol A Biol Sci Med Sci*. 2006;61:1119–1129.
17. Towbin H, Staehelin T, Gordon J. Electrophoretic transfer of proteins from polyacrylamide gels to nitrocellulose sheets: procedure and some applications. 1979. *Biotechnology*. 1992;24:145–149.
18. Gupte AA, Bomhoff GL, Geiger PC. Age-related differences in skeletal muscle insulin signaling: the role of stress kinases and heat shock proteins. *J Appl Physiol*. 2008;105:839–848.
19. Marzetti E, Wohlgemuth SE, Lees HA, Chung HY, Giovannini S, Leeuwenburgh C. Age-related activation of mitochondrial caspase-independent apoptotic signaling in rat gastrocnemius muscle. *Mech Ageing Dev*. 2008;129:542–549.
20. Wheeler MT, Zarnegar S, McNally EM. Zeta-sarcoglycan, a novel component of the sarcoglycan complex, is reduced in muscular dystrophy. *Hum Mol Genet*. 2002;11:2147–2154.
21. Costelli P, Reffo P, Penna F, Autelli R, Bonelli G, Baccino FM. Ca(2+)-dependent proteolysis in muscle wasting. *Int J Biochem Cell Biol*. 2005;37:2134–2146.
22. Chen WS, Xu PZ, Gottlob K et al. Growth retardation and increased apoptosis in mice with homozygous disruption of the Akt1 gene. *Genes Dev*. 2001;15:2203–2208.
23. Zhang Y, Herman B. Ageing and apoptosis. *Mech Ageing Dev*. 2002;123:245–260.
24. Hengartner MO. The biochemistry of apoptosis. *Nature*. 2000;407:770–776.
25. Saraste A, Pulkki K. Morphologic and biochemical hallmarks of apoptosis. *Cardiovasc Res*. 2000;45:528–537.
26. Martin SJ, O'Brien GA, Nishioka WK et al. Proteolysis of fodrin (non-erythroid spectrin) during apoptosis. *J Biol Chem*. 1995;270:6425–6428.
27. Janicke RU, Ng P, Sprengart ML, Porter AG. Caspase-3 is required for alpha-fodrin cleavage but dispensable for cleavage of other death substrates in apoptosis. *J Biol Chem*. 1998;273:15540–15545.
28. Vanags DM, Porn-Ares MI, Coppola S, Burgess DH, Orrenius S. Protease involvement in fodrin cleavage and phosphatidylserine exposure in apoptosis. *J Biol Chem*. 1996;271:31075–31085.
29. Song G, Ouyang G, Bao S. The activation of Akt/PKB signaling pathway and cell survival. *J Cell Mol Med*. 2005;9:59–71.
30. Green AM, Steinmetz ND. Monitoring apoptosis in real time. *Cancer J*. 2002;8:82–92.
31. Cai J, Yang J, Jones DP. Mitochondrial control of apoptosis: the role of cytochrome c. *Biochim Biophys Acta*. 1998;1366:139–149.
32. Goldspink DF, Burniston JG, Tan LB. Cardiomyocyte death and the ageing and failing heart. *Exp Physiol*. 2003;88:447–458.
33. Porter AG, Janicke RU. Emerging roles of caspase-3 in apoptosis. *Cell Death Differ*. 1999;6:99–104.
34. Kwak HB, Song W, Lawler JM. Exercise training attenuates age-induced elevation in Bax/Bcl-2 ratio, apoptosis, and remodeling in the rat heart. *FASEB J*. 2006;20:791–793.
35. Phaneuf S, Leeuwenburgh C. Cytochrome c release from mitochondria in the aging heart: a possible mechanism for apoptosis with age. *Am J Physiol Regul Integr Comp Physiol*. 2002;282:R423–R430.
36. Brown RH, Jr. Dystrophin-associated proteins and the muscular dystrophies. *Annu Rev Med*. 1997;48:457–466.
37. Kirschner J, Bonnemann CG. The congenital and limb-girdle muscular dystrophies: sharpening the focus, blurring the boundaries. *Arch Neurol*. 2004;61:189–199.
38. Malhotra SB, Hart KA, Klamut HJ et al. Frame-shift deletions in patients with Duchenne and Becker muscular dystrophy. *Science*. 1988;242:755–759.
39. Muntoni F, Cau M, Ganau A et al. Brief report: deletion of the dystrophin muscle-promoter region associated with X-linked dilated cardiomyopathy. *N Engl J Med*. 1993;329:921–925.
40. Towbin JA, Bowles KR, Bowles NE. Etiologies of cardiomyopathy and heart failure. *Nat Med*. 1999;5:266–267.
41. Ervasti JM, Campbell KP. A role for the dystrophin-glycoprotein complex as a transmembrane linker between laminin and actin. *J Cell Biol*. 1993;122:809–823.
42. Langenbach KJ, Rando TA. Inhibition of dystroglycan binding to laminin disrupts the PI3K/AKT pathway and survival signaling in muscle cells. *Muscle Nerve*. 2002;26:644–653.
43. Cote PD, Moukhles H, Carbonetto S. Dystroglycan is not required for localization of dystrophin, syntrophin, and neuronal nitric-oxide synthase at the sarcolemma but regulates integrin alpha 7B expression and caveolin-3 distribution. *J Biol Chem*. 2002;277:4672–4679.
44. Sampaolesi M, Yoshida T, Iwata Y, Hanada H, Shigekawa M. Stretch-induced cell damage in sarcoglycan-deficient myotubes. *Pflugers Arch*. 2001;442:161–170.
45. Danialou G, Comtois AS, Dudley R et al. Dystrophin-deficient cardiomyocytes are abnormally vulnerable to mechanical stress-induced contractile failure and injury. *FASEB J*. 2001;15:1655–1657.
46. Rando TA. Role of nitric oxide in the pathogenesis of muscular dystrophies: a "two hit" hypothesis of the cause of muscle necrosis. *Microsc Res Tech*. 2001;55:223–235.

Received June 24, 2009
Accepted December 3, 2009
Decision Editor: Huber R. Warner, MD, PhD